Revista Brasileira de Ciências Ambientais
Brazilian Journal of Environmental Sciences

Synergistic nutrient removal by native microalgae-bacteria consortium: key parameter evaluation

Remoção combinada de nutrientes por um consórcio nativo de microalgas e bactérias: avaliação de parâmetros chave

Thalita Lacerda dos Santos[1], *Felipe Teles Barbosa*[2], *Anna Patricya Florentino*[3], *Gustavo Henrique Ribeiro da Silva*[1]

ABSTRACT

Nutrient bioremediation processes in wastewater are becoming a prevalent focus of research, with microalgae emerging as prominent players. Such microorganisms provide a compelling alternative to traditional sanitation approaches. In light of this emerging interest, the main objective of this study was to explore diverse growth conditions of a native microalgae-bacteria consortium in domestic wastewater, aiming at nutrient bioremediation and biomass production. The investigation was performed on a laboratory scale through Schott® 2.0 L glass bottle photobioreactors, utilizing anaerobically digested wastewater to mitigate its polluting potential effectively. At first, the impact of increasing inflow of CO_2 was evaluated. It was found that the addition of 5% CO_2 yielded the most favorable outcomes, with the remarkable 96.5% of total phosphorus removal within four days alongside a biomass production rate of 0.04 $g.L^{-1}.d^{-1}$. In later steps, variations in light intensity were analyzed, and with 304±3 $\mu mol.m^{-2}.s^{-1}$, yielded the most promising results, with total phosphorus removal of 97.1% within two days and biomass production rate of 0.31 $g.L^{-1}.d^{-1}$. Finally, the influence of temperature was assessed, uncovering 97.2% total phosphorus removal within two days, complemented by a biomass production rate of 0.29 $g.L^{-1}.d^{-1}$. These results facilitated the development of a surface model illustrating the intricate relationship between light and temperature for this consortium. Furthermore, the consortium exhibited remarkable proficiency in nutrient removal from anaerobically digested wastewater, showcasing noteworthy resilience to temperature and light intensity fluctuations.

Keywords: nutrient bioremediation; domestic wastewater treatment, nitrogen and phosphorus removal, regression analysis.

RESUMO

Os processos de biorremediação de nutrientes em águas residuárias tornaram-se um foco predominante de pesquisa, com as microalgas emergindo como atores proeminentes. Esses microrganismos fornecem uma alternativa atraente às abordagens tradicionais de saneamento. Diante do interesse emergente, o principal objetivo deste estudo foi explorar diversas condições de crescimento de um consórcio de microalgas-bactérias nativas em esgoto doméstico, visando a biorremediação de nutrientes e produção de biomassa. A pesquisa foi realizada em escala laboratorial, por meio de fotobiorreatores de vidro Schott® 2,0 L, utilizando esgoto anaerobiamente digerido para mitigar efetivamente seu potencial poluente. A princípio, avaliou-se o impacto do aumento do fornecimento de CO_2. Verificou-se que a adição de 5% de CO_2 produziu os resultados mais favoráveis, com notáveis 96,5% de remoção total de fósforo em quatro dias, juntamente com uma taxa de produção de biomassa de 0,04 $g.L^{-1}.d^{-1}$. Nas etapas posteriores, analisaram-se as variações na intensidade luminosa e, com 304±3 $\mu mol.m^{-2}.s^{-1}$, produziram-se os resultados mais promissores, com remoção total de fósforo de 97,1% em dois dias e taxa de produção de biomassa de 0,31 $g.L^{-1}.d^{-1}$. Por fim, avaliou-se a influência da temperatura, obtendo 97,2% de remoção total de fósforo em dois dias e uma taxa de produção de biomassa de 0,29 $g.L^{-1}.d^{-1}$. Estes resultados permitiram o desenvolvimento de um modelo de superfície que ilustrou a relação intrincada entre luz e temperatura para este consórcio. Além disso, o consórcio exibiu notável proficiência na remoção de nutrientes de esgoto anaerobiamente digerido, apresentando notável resiliência às flutuações de temperatura e intensidade luminosa.

Palavras-chave: bioremediação de nutrientes; tratamento de esgoto doméstico; remoção de nitrogênio e fósforo; análise de regressão.

[1]São Paulo State University – Bauru (SP), Brazil.

[2]University of Natural Resources and Life Sciences – Vienna, Austria.

[3]Wageningen University and Research – Wageningen, Netherlands.

Corresponding author: Thalita Lacerda dos Santos – Department of Civil and Environmental Engineering, São Paulo State University, School of Engineering of Bauru – Av. Engenheiro Luiz Edmundo C. Coube 14-01 – Vargem Limpa – CEP: 17033-360 – Bauru (SP), Brazil. E-mail: thalita.lacerda@unesp.br

Conflicts of interest: the authors declare no conflicts of interest.

Funding: this paper was possible thanks to the scholarship granted from the Coordination for the Improvement of Higher Education Personnel (CAPES), in the scope of the program CAPES-Print, process number 88887.310463/2018-00, mobility number 88887.372663/2019-00 and CAPES – Finance Code 001; National Council for Scientific and Technological Development (CNPq) processes 427936/2018-7 and 308663/2021-7, and the São Paulo Research Foundation (FAPESP) processes 2018/18367-1, and 2022/07475-3 for supporting the development of this study.

Received on: 01/31/2024. Accepted on: 07/16/2024.

https://doi.org/10.5327/Z2176-94781962

Introduction

Technologies based on microalgae-bacteria have emerged as a sustainable option for wastewater treatment (Torres-Franco et al., 2021) with significant emphasis on the importance of the symbiotic relationship between microalgae and bacteria for successful cultivation (Mohsenpour et al., 2021). The interplay of carbon dioxide (CO_2) supply and dioxygen (O_2) production through photosynthesis enhances the efficiency of biochemical oxygen demand removal; in turn, it can reduce aeration costs and contribute to mitigating the adverse effects of excess atmospheric CO_2 (Sutherland and Ralph, 2019; Zhang et al., 2020; Chia et al., 2021; Mohsenpour et al., 2021; Mustafa et al., 2021).

The addition of CO_2 offers numerous advantages in wastewater treatment when utilizing a native microalgae-bacteria consortium (Zhang et al., 2020; Aditya et al., 2022; Yu et al., 2023). One of the effects of CO_2 addition is its impact on potential of hydrogen (pH) value, as in solution, it reacts to form bicarbonate ions (HCO_3^-), which release hydrogen ions (H^+), leading to a reduction in pH values (Kaya et al., 1996; Bernard and Rémond, 2012). For certain microalgae-bacteria consortia, Mohsenpour et al. (2021) showed that there is a strong negative association between pH values and bacterial activity since bacterial activity decreases with the increase in pH (Mohsenpour et al., 2021).

Regarding light intensity, the rate of photosynthetic activity is proportional to the irradiation in cases below the light saturation point (Mohsenpour et al., 2021). Nevertheless, beyond this point, photosynthesis inhibition might arise due to excessive light intensity and elevated temperature, which can adversely affect cell receptors (Gonçalves et al., 2017; Mohsenpour et al., 2021). The optimal light intensity value varies based on species and temperature (Mohsenpour et al., 2021). Maintaining the culture below the saturation point prevents energy loss, as excessive light remains unutilized by the microalgae (Mohsenpour et al., 2021).

Temperature exerts a substantial impact on both growth dynamics and treatment efficiency, but the optimal temperature is contingent upon the specific species under consideration (Mohsenpour et al., 2021). It is generally observed that heightened temperatures correlate with increased metabolic activity, consequently fostering elevated rates of nutrient removal (Gonçalves et al., 2017; Mohsenpour et al., 2021). However, beyond this point, the continuous escalation in temperature leads to a sharp drop in the growth rate (Bernard and Rémond, 2012).

In addition to the aforementioned biochemical issues, the choice of reactor technology significantly impacts the cultivation of microalgae-bacteria consortium once systems can be either open or closed photobioreactors (Torres-Franco et al., 2021; Barboza-Rodríguez et al., 2024). Common open photobioreactors include high-rate algal ponds and conventional stabilization ponds (Torres-Franco et al., 2021). Closed photobioreactors come in multiple configurations, such as tubular and flat, and offer several advantages over open systems, including higher biomass productivity, prevention of gas exchange, and more precise control of variables such as pH, temperature, light intensity, and CO_2 concentration (Torres-Franco et al., 2021; Sirohi et al., 2022). Microalgae biomass production during wastewater treatment can enhance process sustainability by being used as biofertilizer or feedstock for biofuel production. Enclosed photobioreactors protect the cultivation broth from the environment, enabling the generation of high-value products (Alcántara et al., 2020). Despite the high investment and operational costs, these systems achieve high photosynthetic efficiency and volumetric productivity due to their high illuminated surface-to-volume ratio. Although they incur higher energy consumption and capital costs, the high monetary returns from these bioproducts can offset these expenses (Alcántara et al., 2020).

Compared to traditional methods, like anaerobic digestion followed by nitrification and denitrification, which require multiple cycles and extensive infrastructure, microalgae-bacteria consortia offer more efficient nitrogen and phosphorus removal with lower operational costs and less complexity, while chemical methods, though effective, are costly and generate large amounts of contaminated sludge (Gonçalves et al., 2017).

Furthermore, wastewater treatment employing microalgae holds the potential to substantially contribute to mitigating other escalating societal challenges, including water scarcity which impacts up to 40% of the global population, and the escalating risk of food insecurity due to the expanding global population (Wali et al., 2021). In some regions, the depletion of phosphorus reserves has already exacerbated these concerns (Wali et al., 2021). It is paramount to underscore that phosphorus is indeed a finite resource (Wali et al., 2021).

Therefore, addressing concerns related to water quality preservation, mitigation of environmental hazards like eutrophication and water scarcity, and the increasing demand for macro and micronutrients in agriculture, there is a critical need for research and development of technologies focused on nutrient extraction, recovery, and reuse from common sources such as domestic wastewater. This study evaluated how varying CO_2 supplementation, light intensity, and temperature affect nutrient removal and biomass generation potential in a native microalgae-bacteria consortium thriving in treated domestic effluent within an upflow anaerobic biological filter.

The study aimed to analyze the behavior of this consortium under controlled conditions and assess its potential for future applications. A systematic experimentation approach was employed to develop regression models predicting nutrient removal based on specific CO_2 levels and light intensities, in order to streamline future experimental protocols and resource allocation.

Materials and Methods

Microalgae culture and culturing medium

The microalgae-bacteria consortium used in this study was obtained through the enrichment of the native community of

secondary effluent from a local municipal wastewater treatment plant (MWTP), located in the city of Bauru, São Paulo, Brazil (22°13´39.707"S, 49°12´44.829" W). This enrichment was performed in 1.0 L Erlenmeyer's (operational volume), and an aliquot of the native consortium in the early stationary phase was used in a series of 10% (v/v) inoculation to the natural effluent. Cultivation for enrichments was kept in an acclimatized room at 24°C standard deviation (±) 2°C and 154±2 $\mu mol.m^{-2}.s^{-1}$ of light intensity, with a 12/12 h light/dark cycle. The secondary effluent directly used as the medium for consortium growth was collected in the upflow anaerobic biological filter of the MWTP.

The effluent used as the medium for consortium growth was collected from the outlet of an upflow anaerobic biological filter at an MWTP, located in Bauru (22°13´39.707"S, 49°12´44.829" W). The plant comprised screening, grit removal, primary settling, an upflow anaerobic biological filter, constructed wetlands, and polishing ponds. The microalgae-bacteria consortium used in this study was obtained through the enrichment of the native community in the secondary effluent. This enrichment was performed in 1.0 L Erlenmeyer's, with an aliquot of the native consortium in the early stationary phase used for a series of 10% (v/v) inoculation to the effluent. The cultures for enrichment were maintained in a climate-controlled room at 24±2°C, with a light intensity of 154±2 $\mu mol.m^{-2}.s^{-1}$, and a 12/12 h light/dark cycle.

The primary average parameters of the utilized effluent are delineated in Table 1.

Experimental set-up

Three investigations were conducted to evaluate the impact of CO_2 enrichment, light intensity, and temperature variations on the activity of the native microalgae-bacteria consortium for nitrogen and phosphorus removal (Figure 1).

Rounded Schott® 2.0 L glass reactors were inoculated with 10% (v/v) of native microalgae-bacteria consortium in the recent stationary phase, with an initial concentration of approximately 10^6 $cells.mL^{-1}$. The reactors were equipped with an aeration system comprising an air compressor (Direct Air G3, Chiaperini), a CO_2 cylinder, and flow meters with a control range of 0–3 $L.min^{-1}$ (RWR, São Paulo, Brazil). The aeration was maintained at a constant rate of 1.0 $L.min^{-1}$ throughout all experiments.

Light intensity was provided by horizontally arranged LED lamps (Brilia 300194, 3000 K) and LED strips (120 LEDS, 6000 K), during a photoperiod of 12/12 hours. The light intensity was measured using an infrared gas analyzer model LCpro-SD (ADC Bioscientific™, Hoddesdon, England). Temperature control was achieved through air conditioning, and temperature was monitored using a datalogger sensor (Hobo™ UA-002-64, ONSET).

Batch cultures and sampling

Investigation 1 — Influence of carbon dioxide concentration

The addition of CO_2 offers several benefits in wastewater treatment using a native microalgae-bacteria consortium (Beltrán-Rocha et al., 2017). The crucial relationship between microalgae and CO_2 in photosynthesis is that low CO_2 levels can hamper growth rates and nutrient removal, while high CO_2 concentrations can enhance microalgal growth (Kaya et al., 1996; Mohsenpour et al., 2021).

To assess the impact of CO_2 increase, three consecutive treatments were conducted separately in individual batch mode. In Treatment I, compressed air without CO_2 enrichment was used, and constant forced aeration was applied using glass rods with porous diffusers at the end, with an airflow rate of 1.0 $L.min^{-1}$ per reactor.

Following a study by Liu et al. (2017), Treatment II involved enriching the compressed air with 5% CO_2, while Treatment III involved enriching the compressed air with 10% CO_2. The total airflow rate of 1.0 $L.min^{-1}$ per reactor was maintained across all experiments. The cultivation took place in a controlled environment, keeping consistent parameters across all groups. Analysis of nutrient removal and biomass production rates across the three treatments was undertaken to identify the optimal condition. The most effective condition identified from these experiments was utilized in Investigation 2.

Investigation 2 — Light intensity

Based on the optimal CO_2 concentration determined in Investigation 1, two additional treatments were conducted in Investigation 2 to test different light-intensity conditions. In Treatment IV, the light intensity was increased from 154±2 $\mu mol.m^{-2}.s^{-1}$ to 211±3 $\mu mol.m^{-2}.s^{-1}$. In Treatment V, the light intensity was set at 304±3 $\mu mol.m^{-2}.s^{-1}$.

Table 1 – Characterization of the effluent from a municipal wastewater treatment plant.

Parameter	Mean±SEM	Methodology
pH	7.1±0.1	4500-HB (measurement by portable probe)
COD ($mg.L^{-1}.O_2$)	185.3±42.5	COD TNT® reagent kit Hach
TN ($mg.L^{-1}$)	34.8±1.1	DR/5000 Hach Pillow Kit and Hach HQ-40d Multiparameter Meter
TP ($mg.L^{-1}$)	4.3±0.3	Total phosphorus TNT® reagents Hach kit
Dissolved oxygen ($mg.L^{-1}$)	1.2±0.6	Method 4500-O (measurement by portable probe)

SEM: standard error of the mean; pH: potential hydrogen; COD: chemical oxygen demand; TN: total nitrogen; TP: total phosphorus.

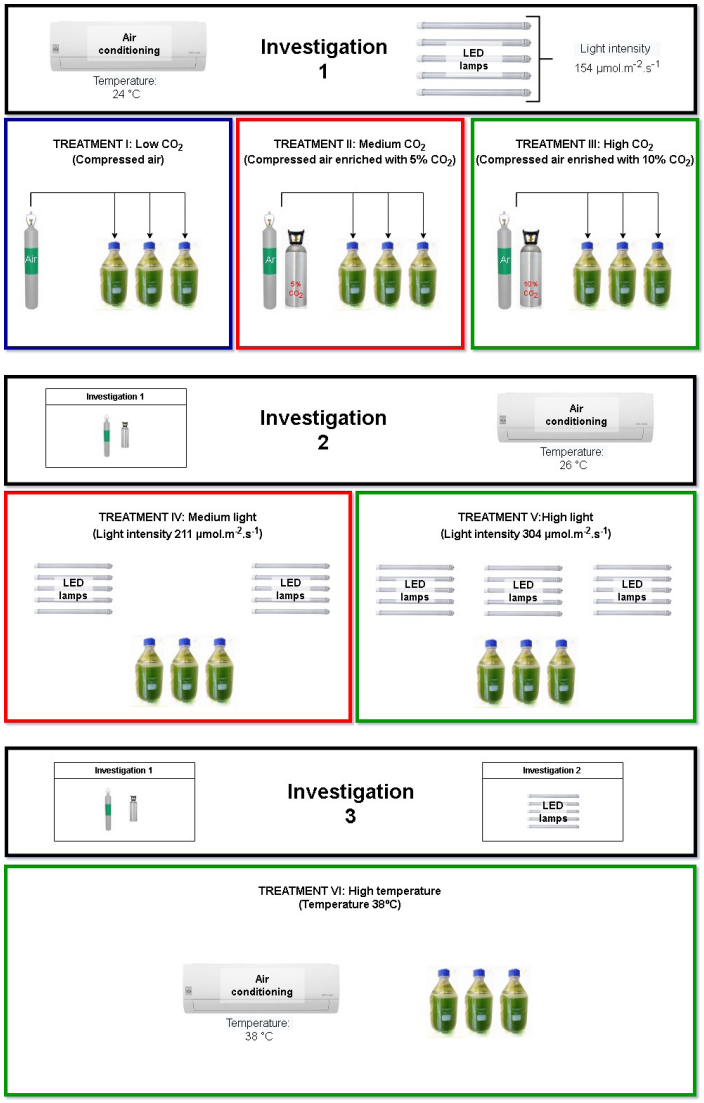

Figure 1 – Flowchart of the experimental setup.

Light intensity significantly influences the balance of mixed communities, creating an environment where microalgae growth surpasses that of bacteria, especially when nutrients become scarce and competition among species intensifies (Mohsenpour et al., 2021).

Several authors associate increased biomass production with elevated light intensity, up to a certain threshold (Li et al., 2012; Delgadillo-Mirquez et al., 2016; Lee and Lei, 2019; Silva et al., 2019). Consequently, there exists a saturation point of light intensity, which varies with temperature and species, below which the rate of photosynthetic activity aligns proportionally with light intensity and, when light intensity exceeds this point, photoinhibition may occur (Mohsenpour et al., 2021).

The nutrient removal and biomass production rates were assessed for each experiment, and the most effective condition was employed in Investigation 3.

Investigation 3 — Temperature increase

According to Kube et al. (2018), the impact of temperature on algae varies between species. While many algal species exhibit accelerated growth rates and nutrient removal with rising temperature, it is important to recognize that temperature differentially influences nitrogen and phosphorus removal (Kube et al., 2018). Furthermore, cultivating microalgae at lower temperatures necessitates the employment of lower light intensities to mitigate photoinhibition; in addition, it offers operational benefits, encompassing heightened oxygen solubility and the constraint of growth rates among competing microorganisms (Mohsenpour et al., 2021). Building upon the optimal CO_2 concentration determined in Investigation 1 and the optimal light intensity determined in Investigation 2, a new set of cultivation was conducted to evaluate the effects of temperature. In Treatment VI (High T), the temperature was set at 38±5°C. Nutrient removal and biomass production rates were evaluated under these conditions.

Analytical procedure

On a daily basis, a 50 mL sample was collected for physical-chemical and biological analyses. The collected samples were promptly analyzed for pH, dissolved oxygen, alkalinity, and optical density measurements in each reactor to ensure accurate and timely data acquisition. Optical density was measured using a spectrophotometer (Nanocolor™ UV/VIS II, Macherey-Nagel, Germany) at wavelengths of 530, 680, and 750 nm (Silva et al., 2020; Pompei et al., 2023).

Samples were filtered by a glass fiber membrane (GF5, Ø 0.4µm, Macherey-Nagel, Duren, Germany) to measure dissolved nutrients—total nitrogen (TN), nitrate (NO_3-N), total Kjeldahl nitrogen (TKN), and total phosphorus (TP)—as well as chemical oxygen demand (COD). TN, NO_3-N, and TKN were quantified using the tube test TKN 16 (Nanocolor, Munich, Germany). TP, total suspended solids (TSS), and COD were quantified according to Standard Methods 4500-P, 2540, and 5220-D, respectively (APHA, 2012).

All analyses were conducted at the Laboratory of Environmental Sanitation within the Department of Civil and Environmental Engineering at the São Paulo State University in Bauru, São Paulo.

Productivity, efficiency of conversion, and removal rates

Productivity rate ($g.L^{-1}.d^{-1}$) is given by a relationship with TSS, according to Equation 1 (Pompei et al., 2023):

$$P = \frac{X_1 - X_0}{t_1 - t_0} \quad (1)$$

Where:

X_1 = highest biomass value measured in a batch ($g.L^{-1}$);

X_0 = initial value of biomass measured in a batch ($g.L^{-1}$);

t_1 = time (d) where the highest biomass value measured in a batch occurred; and

t_0 = initial time (d) for a batch.

To evaluate the impact on biomass of light intensity, the efficiency of conversion of light intensity into biomass produced was calculated as follows in Equation 2 (Li et al., 2012):

$$Conversion\ efficiency = \frac{X}{I} \quad (2)$$

Where:

X = highest accumulated biomass concentration ($g.L^{-1}$) obtained during the experiment; and

I = intensity of light ($\mu mol.m^{-2}.s^{-1}$) applied during the experiment.

Let i = N, P denote, respectively, nitrogen and phosphorus. The removal rate R_i ($mg.L^{-1}.d^{-1}$) for a nutrient i is calculated according to Equation 3 (Delgadillo-Mirquez et al., 2016):

$$R_i = \frac{S_{i0} - S_{if}}{t_{95}} \quad (3)$$

Where:

S_{i0} = initial concentration of a nutrient i;

S_{if} = final concentration of the corresponding nutrient; and

t_{95} = time in which phosphorus removal was greater than or equal to 95% S_{p0} (initial phosphorus concentration).

Statistical analysis

Prior to performing statistical analyses, a pre-processing of the data was performed. To do so, let Y_t represent the values of a chemical compound, e.g., phosphorus, in the time t and a collection of $\{Y_t, 0 \leq t \leq t_{max}\}$ represent a time series for Y. Given that the initial condition of each replicate of each treatment has a different value, the concentration of a variable Y_t ($mg.L^{-1}$) was divided by its initial value Y_0 ($mg.L^{-1}$) for each time t. In other words, the original time series $\{Y_0, Y_1, \ldots, Y_{tmax-1}, Y_{tmax}\}$ became $\left\{1, \frac{Y_1}{Y_0}, \ldots, \frac{Y_{tmax-1}}{Y_0}, \frac{Y_{tmax}}{Y_0}\right\}$ for $Y_0 > 0$. For all statistical analyses, three replicates per experimental condition per time were available and all statistical methods presented in this paper were implemented in R (RStudio, 2020) software.

Concentration-time plots

To evaluate the dynamics of phosphorus concentration over the bioprocess time, mean±standard errors were plotted for each treatment and time point, considering the investigations described above. Moreover, three kinetic variables were calculated for each replicate of each treatment to assist in the comparison of different treatments: area under the concentration-time curve from 0–4 days ($AUC_{[0,4]}$), area under the concentration-time curve from 0–7 days ($AUC_{[0,7]}$), and t_{95}.

In order to estimate the area under the curve (AUC) from 0 to t ($AUC_{[0,t]}$), where $0 \leq t \leq t_{max}$, let us define a sequence of time points $\{t_0, t_1, \ldots, t_{max}\}$, and let the AUC be defined as in Equation 4:

$$AUC_{[0,\underline{t}]} = \int_0^{\underline{t}} Y_t \, dt. \quad (4)$$

The trapezoidal rule was used to compute values for the AUC given by Equation 4.

Differences between treatments

A linear model was used to investigate if different treatments had significant effects on $AUC_{[0,4]}$, $AUC_{[0,7]}$, and t_{95}. The general formulation of the model is given by Equation 5:

$$Z = S\beta + \varepsilon, \quad (5)$$

Where:

Z = vector containing values for $AUC_{[0,4]}$, $AUC_{[0,7]}$, or t_{95};

S = treatment matrix;

β = vector containing the coefficients for each treatment; and

$\varepsilon \sim N(0, \sigma^2)$ = error vector with a normal distribution with mean zero and variance σ^2.

When fitting the linear model in Equation 5, if the p-value of the fitting is smaller than a significance level α=0.05, the variability of Z can be explained by differences among treatments described by the matrix S. The variability of Z was analyzed via analysis of variance (ANOVA) from the results obtained by fitting Equation 5.

Furthermore, the Tukey's honestly significance difference (Tukey's HSD) test was performed as a *post-hoc* analysis to quantify the difference between two treatments pairwise when the p-value from ANOVA is smaller than α=0.05. All numerical results are displayed in this paper with two decimal places and E-xx denotes 10^{-xx}.

Results and Discussion

Influence of carbon dioxide concentration

The treatments I, II, and III showed that the introduction of varying levels of additional CO_2 stimulates distinct bioprocess dynamics. The daily nutrient removal rates, calculated according to Equation 3, are presented in Table 2, with Treatment II achieving the most favorable nutrient removal rates. Notably, Treatment I achieved a TN removal rate 26% higher than Treatment III.Regarding TN, the removal rate was 84% for Treatment I, which displayed the highest pH value of 8.07, 87% for Treatment II, and 90% for Treatment III, with the lowest pH value of 5.96. Nitrogen removal rates can be attributed to culture growth and abiotic phenomena like ammonia volatilization, related to high pH values resulting from photosynthetic activity and denitrifying bacteria respiration (Delgadillo-Mirquez et al., 2016). The TN removal in Treatment I could be attributed to both biotic and abiotic factors, including ammonia volatilization, which could have positively influenced the total nitrogen removal.

Regarding phosphorus, its bioavailability is notably influenced by pH, tending to precipitate at levels greater than 9.0 (Beltrán-Rocha et al., 2017). As illustrated in Figure 2, at approximately seven days of bioprocessing, TP removal achieved similar mean levels for all tested treatments.

To determine whether or not there was a difference due to treatments, the linear regression model given by Equation 6 was fitted to $AUC_{[0,4]}$, $AUC_{[0,7]}$, and t_{95}. Results of ANOVA for all kinetic variables are presented in Table 3.

Table 2 – Description of the treatments carried out in the experiment.

Treatment	TN removal mg/L/d	NO_3-N mg/L/d	TKN removal mg/L/d	Final pH
I (Air)	4.77	4.53	0.23	8.11±0.05
II (5% CO_2)	7.42	7.01	0.31	6.28±0.04
III (10% CO_2)	3.78	3.61	0.17	5.92±0.06

TN: total nitrogen; NO_3-N: nitrate; TKN: total Kjeldahl nitrogen; pH: potential hydrogen; CO_2: carbon dioxide; ±: standard deviation.

Since effects of treatments can explain the variability of $AUC_{[0,4]}$, $AUC_{[0,7]}$, and t_{95}, a *post-hoc* test was performed to quantify the differences between treatments pairwise. Results are shown in Table 4.

No significant difference was found between Treatments II and I for AUC, implying that these two treatments have similar properties regarding TP removal. Furthermore, the time to reach 95% TP removal significantly differed for II *versus* I and III *versus* II. Treatment III took 2.66 days more than Treatment II to achieve the same removal percentage. In Treatment II, there was 95% TP removal 3.66 days before Treatment I. In this sense, among the treatments tested, Treatment II obtained the highest percentages of nutrient removal and the best growth profile, achieving a TSS production rate of 0.07 $g.L^{-1}.d^{-1}$, which is considered the best condition.

Nevertheless, it is vital to underscore that aeration, whether CO_2-enriched or not presents a substantial cost challenge in operating these systems (Mohsenpour et al., 2021). By utilizing emissions from industrial process units and municipal wastewater as inputs for cultivating microalgae, there is significant potential for reducing CO_2 emissions and lowering costs in microalgae biomass production (Beltrán-Rocha et al., 2017). This approach not only addresses environmental challenges but also optimizes resource utilization, providing valuable opportunities for sustainable practices. Another advantage of enriching the system with CO_2 is its potential to remove pathogens (e.g., *Pseudomonas aeruginosa*) and total coliform, thereby enhancing the overall safety and quality of the microalgae treatment process (Ruas et al., 2018).

Influence of light intensity and temperature

The biomass production increased with light intensity in terms of TSS. Treatment II yielded a TSS of 0.46±0.04 $g.L^{-1}$, while Treatment IV demonstrated a TSS of 1.51±0.01 $g.L^{-1}$, marking an increase of approximately 230%. Treatment V yielded a TSS of 2.11±0.01 $g.L^{-1}$, a substantial increase of around 360% compared to Treatment II.

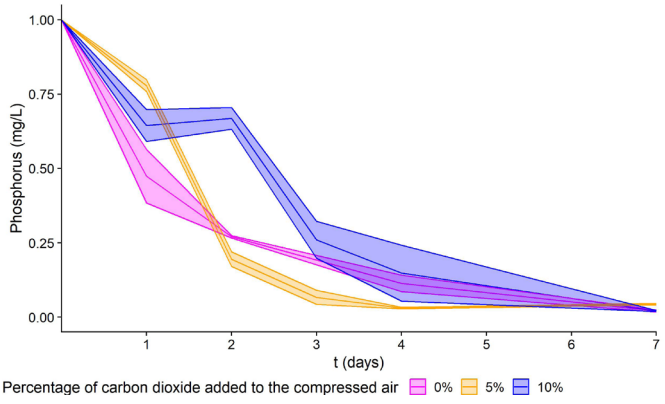

Figure 2 – Mean and standard error of the mean for total phosphorus at different carbon dioxide levels.

Table 3 – Analyses of variance to compare different levels of carbon dioxide.

	Source of information	Degrees of freedom	Sum of squares	Mean square	F-value	p-value
$AUC_{[0,4]}$	Treatments	3	27.77	9.26	302.06	6.21E-07
	Residuals	6	0.18	0.03		
$AUC_{[0,7]}$	Treatments	3	34.21	11.40	124.35	8.62E-06
	Residuals	6	0.55	0.09		
t_{95}	Treatments	3	287.63	95.88	85.08	2.63E-05
	Residuals	6	6.76	1.13		

AUC: area under the concentration-time curve [days]; t_{95}: time in which phosphorus removal was greater than or equal to 95% $S_{p\,0}$ (initial phosphorus concentration).

Table 4 – Tukey's test to compare different levels of carbon dioxide addition.

	Treatment comparison	Difference	95% confidence interval	adjusted p-value
$AUC_{[0,4]}$	II *vs* I	0.06	(-0.38, 0.50)	0.90
	III vs I	0.65	(0.22, 1.09)	0.01
	III *vs* II	0.59	(0.15, 1.03)	0.01
$AUC_{[0,7]}$	II *vs* I	-0.03	(-0.79, 0.73)	0.99
	III *vs* I	0.71	(-0.05, 1.46)	0.07
	III *vs* II	0.73	(-0.03, 1.49)	0.06
t_{95}	II *vs* I	-3.66	(-6.32, -1.00)	0.01
	III *vs* I	-0.99	(-3.66, 1.66)	0.52
	III *vs* II	2.66	(0.00, 5.32)	0.05

AUC: area under the concentration-time curve [days]; t_{95}: time in which phosphorus removal was greater than or equal to 95% $S_{p\,0}$ (initial phosphorus concentration).

Table 5 – Comparison between light intensity conversion efficiency values into biomass.

Experiment	Light intensity (µmol/m²/s)	Conversion efficiency (g/L)/(µmol/m²/s)	Reference
Chlorella kessleri[a]	120	0.0117	(Li et al., 2012)
	200	0.0066	(Li et al., 2012)
Chlorella protothecoide[1]	120	0.0071	(Li et al., 2012)
	200	0.0053	(Li et al., 2012)
Treatment II[b]	154	0.0035	This study
Treatment IV[b]	211	0.0077	This study
Treatment V[b]	304	0.0073	This study

[a]Pure culture in sterilized centrate media.
[b]Native consortium of microalgae and bacteria in anaerobically digested wastewater.

The values of light intensity conversion into biomass production, calculated according to Equation 2, are summarized in Table 5. The biomass conversion efficiency increased along with the light intensity, while for the pure cultures studied by Li et al. (2012), the conversion efficiency decreased with increasing light intensity.In the context of this study, the increase in light intensity up to these values resulted in increased conversion efficiency in the case of Treatment II. Conversely, Treatment V displayed a reduction in conversion efficiency, aligning with observations in a study by Li et al. (2012).

The rise in light intensity and temperature led to an increase in TP removal rate within Treatment VI compared to the Investigations 1 and 2, shown in Figure 3. Normalized concentrations of TP during the bioprocess were shown to be very homogeneous among the replicates.

Visually, the decrease in TP concentration stabilized at around four days of bioprocess reaching similar percentages of TP removal for all tested treatments. Approximately on the seventh day of the experiment, the removal rate of the bioreactors treated at 154 µmol $m^{-2}.s^{-1}$ was slightly higher than the other conditions tested. To determine whether there was a significant difference due to treatment effects, the linear regression model given by Equation 6 was fitted to $AUC_{[0,4]}$, $AUC_{[0,7]}$, and t_{95}. Results of ANOVA for all kinetic variables are presented in Table 6.

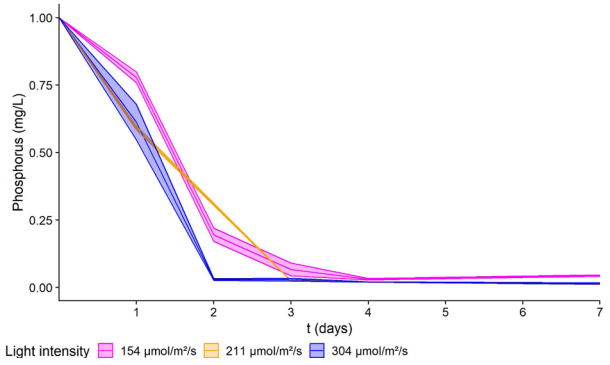

Figure 3 – Mean and standard error of the mean for total phosphorus for different light intensity.

Analogously to the analysis performed for CO_2, since different levels of light intensity can explain the variability of $AUC_{[0,4]}$, $AUC_{[0,7]}$, and t_{95}, a *post-hoc* test was performed to quantify the differences between treatments pairwise. Results are shown in Table 7.

The comparison revealed that higher light intensities promoted a lower AUC (for both the fourth and seventh days) and a lower time to reach 95% TP removal. Regarding the AUC during the total bioprocess time, Treatment V achieved 95% removal in 1.28 and 0.91 days on average, sooner than Treatments II and IV, respectively.

Table 6 – Analysis of variance to compare different levels of light intensity.

	Source of information	Degrees of freedom	Sum of squares	Mean square	F-value	p-value
$AUC_{[0,4]}$	Treatments	3	17.61	5.87	775.87	3.71E-08
	Residuals	6	0.05	0.01		
$AUC_{[0,7]}$	Treatments	3	19.46	6.49	890.66	2.46E-08
	Residuals	6	0.04	0.01		
t_{95}	Treatments	3	72.21	24.07	245.10	1.16E-06
	Residuals	6	0.59	0.10		

AUC: area under the concentration-time curve [days]; t_{95}: time in which phosphorus removal was greater than or equal to 95% $S_{p\,0}$ (initial phosphorus concentration).

Table 7 – Tukey's test to compare different levels of light intensity.

	Comparison	Difference	95% confidence interval	Adjusted p-value
$AUC_{[0,4]}$	IV *vs.* II	-0.12	(-0.34, 0.10)	0.28
	V *vs.* II	-0.38	(-0.59, -0.16)	0.00
	V *vs* IV	-0.25	(-0.47, -0.04)	0.03
$AUC_{[0,7]}$	IV *vs.* II	-0.19	(-0.40, 0.03)	0.08
	V *vs.* II	-0.44	(-0.65, -0.22)	0.00
	V *vs.* VI	-0.25	(-0.46, -0.04)	0.03
t_{95}	IV vs II	-0.38	(-1.16, 0.41)	0.38
	V vs II	-1.28	(-2.07, -0.50)	0.01
	V vs VI	-0.91	(-1.70, -0.13)	0.03

AUC: area under the concentration-time curve [days]; t_{95}: time in which phosphorus removal was greater than or equal to 95% $S_{p\,0}$ (initial phosphorus concentration).

The percentage removal values for phosphorus obtained in Investigation 2 and under the best condition of Investigation 1 were compared with experiments conducted on a pure culture of *Chlorella vulgaris* by Mayhead et al. (2018), as illustrated in Table 8. Mixed cultures of microalgae and bacteria were shown to be the most viable option for effluent treatment, given the challenges associated with sustaining a pure culture. This was evidenced by the observed reduction in the growth rate of the pure culture of *C. vulgaris* in effluent that had not undergone autoclaving and filtration. Concerning temperature, mean, and standard error of phosphorus for time points and across all replicates of a treatment is plotted in Figure 4.

Exposure to Treatments IV and VI generated homogenous results for each time point and it seems that both treatments achieved similar TP removal at the end of the process. A linear regression, as given by Equation 6, was fitted to $AUC_{[0,4]}$ and t_{95}, given that after four days of bioprocess, there was dead biomass for some experiments. The results of ANOVA for all kinetic variables are presented in Table 9.Since variability of the response variable can certainly be explained by treatment effects, the following table outlines the results of the *post-hoc* test to compare treatment mean effects (Table 10).

When comparing both kinetic variables, high temperatures showed a smaller average AUC and were almost one day faster to remove 95% of the TP. According to the performed analyses, the best treatment to remove TP was at high temperatures.

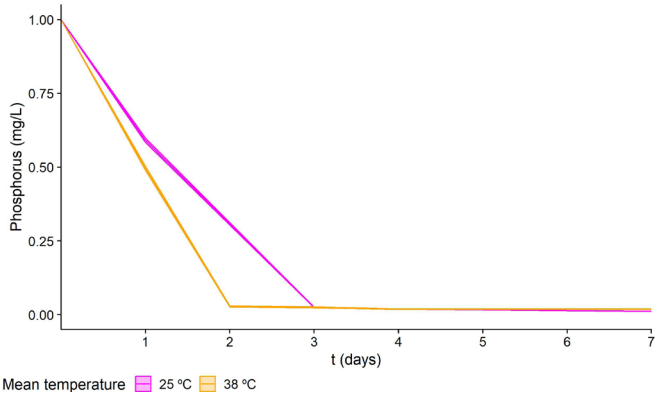

Figure 4 – Mean and standard error of the mean for total phosphorus for different temperature.

It is important to highlight that light and temperature analyses shown in the previous tables concerned only one variable at a time since either temperature (for light experiments) or light was constant (for temperature experiments). Using collected data from all the experiments carried out under 5% CO_2, the following linear model was proposed to summarize the relationship between temperature, light intensity, and phosphorus removal percentage:

$$Removal = \beta_1 Light + \beta_2 Temperature + \beta_3 Light^2 + \beta_4 Temperature^2 + \varepsilon. \quad (6)$$

Moreover, the maximum theoretical removal (*Removal**) is given by:

$$Removal^* = \beta_1 Light^* + \beta_2 Temperature^* + \beta_3 Light^{*2} + \beta_4 Temperature^{*2} \quad (7)$$

Where *Light** and *Temperature** are the solutions for the following equation:

$$\nabla Removal = 0 \Rightarrow \begin{cases} \beta_1 + 2\beta_3 Light^* = 0 \\ \beta_2 + 2\beta_4 Temperature^* = 0 \end{cases} \quad (8)$$

Where $\nabla Removal$ is the gradient of Equation 6 with respect to the variables *Light* and *Temperature*.

In other words, when solving the gradient problem stated by Equation 8, it is possible to find the direction of maximum removal given by the parameter estimates.

Table 8 – Comparison between light intensity and percentage of phosphorus removal.

Experiment	Growing media	Light intensity (μmol/m²/s)	% Phosphorus	Reference
Chlorella vulgaris[a]	F2P[c]	177	90 PO_4-P	(Mayhead et al., 2018)
Chlorella vulgaris[a]	Primary effluent (filtered and autoclaved)	177	98 PO_4-P	(Mayhead et al., 2018)
Chlorella vulgaris[a]	Primary effluent	177	97 PO_4-P	(Mayhead et al., 2018)
Treatment II[b]	Secondary effluent	154	96 P_{total}	This study
Treatment IV[b]	Secondary effluent	211	97 P_{total}	This study
Treatment V[b]	Secondary effluent	304	97 P_{total}	This study

[a]Pure culture in sterilized centrate media.
[b]Native consortium of microalgae and bacteria in anaerobically digested wastewater.
[c]F2P is an optimized medium used as a control in the experiment
PO_4-P: orthophosphate as phosphorus; P: phosphorus.

Table 9 – Analysis of variance to compare different levels of temperature.

	Source of information	Degrees of freedom	Sum of squares	Mean square	F-value	p-value
$AUC_{[0,4]}$	Treatments	2	9.53	4.77	18908.23	1.12E-08
	Residuals	4	0.00	0.00		
t_{95}	Treatments	2	37.95	18.98	103548.47	3.73E-10
	Residuals	4	0.00	0.00		

AUC: area under the concentration-time curve [days]; t_{95}: time in which phosphorus removal was greater than or equal to 95% $S_{p\,0}$ (initial phosphorus concentration).

Table 10 – Tukey's test to compare different levels of temperature.

	Treatment comparison	Difference	95% Confidence interval	adjusted p-value
$AUC_{[0,4]}$	VI *vs* IV	-0.38	(-0. 14, -0.34)	9.94E-06
t_{95}	VI *vs* IV	-0.99	(-1.02, -0.96)	1.14E-13

AUC: area under the concentration-time curve [days]; t_{95}: time in which phosphorus removal was greater than or equal to 95% $S_{p\,0}$ (initial phosphorus concentration).

Table 11 – Summary statistics of regression model for total phosphorus removal ($R^2 \approx 1.0$).

Parameter	Estimate	Standard error	t-value	p-value
β_1	2.20E-01	1.80E-02	12.24	1.85E-06
β_2	4.85	1.24E-01	39.02	2.04E-10
β_3	-4.43E-04	3.84E-05	-11.55	2.87E-06
β_4	-7.84E-02	1.87E-03	-41.93	1.15E-10

Estimates of Equation 6, when using collected data, are outlined in Table 11, where the coefficient of determination for removal explained by light and temperature is close to 1 (one). This means that, with the collected data from the experiments in this research, the variability of the proportion of removal can be explained almost 100% by a linear combination of light intensity and temperature. The plot in Figure 5 was created by applying the estimates provided in Table 11 (Equation 6), where the green dot above the surface corresponds to the theoretical maximum point, given by the solution of Equation 8: (*Light**, *Temperature**, *Removal**) = (247.67, 30.94, 102.22). Note that the identified maximum value exceeds 100%, contradicting the biological aspects of the process; therefore, we refer to it as a theoretical maximum point. However, it is important to highlight that light and temperature conditions equal or close to *Light** and *Temperature**, respectively, promote the achievement of high levels of removal in practice.

Moreover, applying the same procedure for nitrogen removal, the following linear model was proposed to summarize the relationship between temperature, light intensity, and nitrogen removal percentage:

$$Removal = \beta_5 Light + \beta_6 Temperature + \beta_7 Light^2 + \beta_8 Temperature^2 + \varepsilon. \quad (9)$$

Analogously to the procedure in Equations 7 and 8, the maximum theoretical removal of nitrogen (*Removal**) is given by:

$$Removal^* = \beta_5 Light^* + \beta_6 Temperature^* + \beta_7 Light^{*2} + \beta_8 Temperature^{*2}, \quad (10)$$

Where *Light** and *Temperature** are the solutions for the following equation:

$$\nabla Removal = 0 \Rightarrow \begin{cases} \beta_5 + 2\beta_7 Light^* = 0 \\ \beta_6 + 2\beta_8 Temperature^* = 0 \end{cases} \quad (11)$$

Estimates of Equation 9, when using collected data, are outlined in Table 12.The plot in Figure 6 was created based on the estimates provided in Table 12 (Equation 10), where the green dot above the surface is the theoretical maximum point, given by the solution of Equation 11: (*Light**, *Temperature**, *Removal**) = (203.29, 31.56, 99.54).

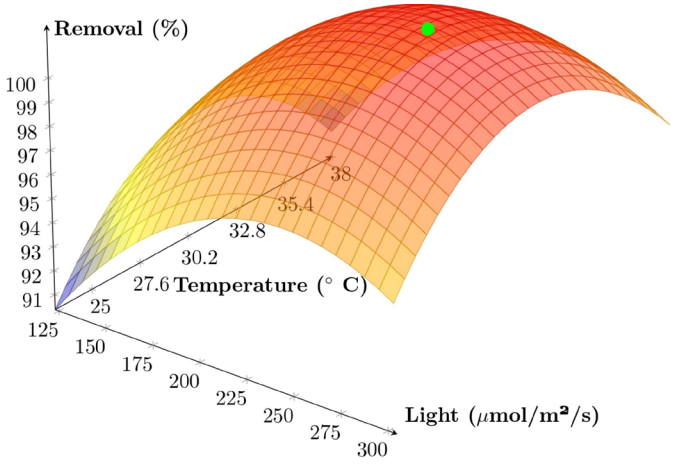

Figure 5 – Prediction surface of regression model: removal of total phosphorus under medium addition of carbon dioxide. Green point refers to theoretical maximum removal.

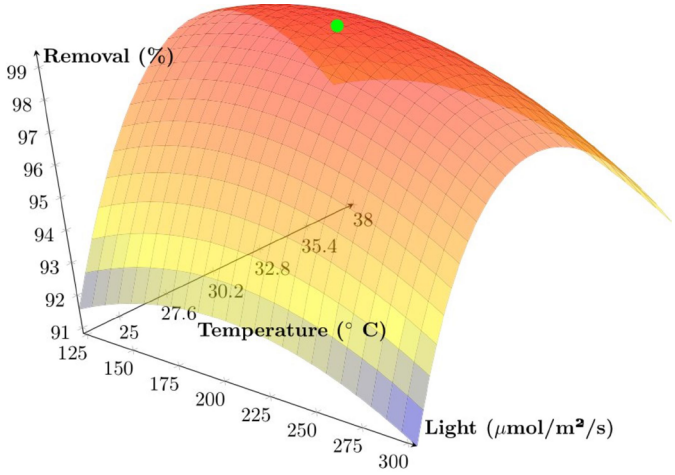

Figure 6 – Prediction surface of regression model: total nitrogen removal under medium addition of carbon dioxide. Green point refers to theoretical maximum removal.

Table 12 – Summary statistics of regression model for nitrogen removal ($R^2 \approx 0.9998$).

Parameter	Estimate	Standard error	t-value	p-value
β_5	0.08	0.07	1.14	0.28
β_6	5.81	0.45	12.81	1.58E-07
β_7	-1.91E-04	1.49E-04	-1.28	0.23
β_8	-0.09	0.01	-13.66	8.59E-08

Conclusion

Based on the outcomes of this study, it can be deduced that the native mixed microalgae-bacteria culture demonstrated excellent performance in anaerobic effluent treatment, suggesting its viability as a potential post-treatment solution. Among the parameters examined, CO_2 supplementation significantly influenced microalgae development, leading to increased biomass production. Its integration, however, imposes additional costs to full-scale operations. Additionally, higher light intensity had positive effects on both nutrient removal and biomass production, making it particularly advantageous for implementation in regions characterized by high light intensity, such as Brazil. Similarly, elevated temperature also proved beneficial for the native microalgae-bacteria consortium employed in this study.

Therefore, it can be inferred that the native microalgae-bacteria consortium demonstrates proficiency in nutrient removal, resilience to temperature fluctuations, and tolerance to light intensity. The encouraging and promising results obtained at the laboratory scale strongly indicate the potential for successful piloting of this community in larger-scale experiments and integration with other effluent treatment processes. Moreover, the biomass produced could be extensively explored as a substrate for biotechnological products, potentially revolutionizing applications in agriculture or biofuel production, pending thorough assessment of lipid accumulation.

Acknowledgements

The authors would like to acknowledge the support obtained from the following Brazilian institutions: National Council for Scientific and Technological Development (CNPq) projects 427936/2018-7, 308663/2021-7, and 309064/2018-0); Coordination for the Improvement of Higher Education Personnel (CAPES) for the Young Talented Researcher grant awarded to Anna Patricya Florentino (88887.372663/2019-00) during the Institutional Program for Internationalization (PRINT); and CAPES – Finance Code 001; and the São Paulo Research Foundation (FAPESP) process 2018/18367–1.

Authors' Contributions

Santos, T.L.: conceptualization, data curation, formal analysis, investigation, methodology and, writing – original draft. **Teles Barbosa**, F.: data curation, formal analysis, investigation, methodology, software, supervision, validation, visualization and, writing – original draft. **Florentino**, A.P.: conceptualization, data curation, formal analysis, investigation, methodology, supervision, validation, visualization and, writing – review & editing. **Silva**, G.H.R.: conceptualization, funding, acquisition, investigation, methodology, project administration, resources, supervision, validation, visualization, writing – review & editing.

References

Aditya, L.; Mahlia, T.M.I.; Nguyen, D.D.; Nguyen, L.N.; Vu, H.P.; Nghiem, L.D., 2022. Microalgae-bacteria consortium for wastewater treatment and biomass production. Science of The Total Environment, v. 838 Part 1, 155871-155871. https://doi.org/10.1016/j.scitotenv.2022.155871.

Alcántara, C.; De Godos, I.; Muñoz, R., 2020. Wastewater treatment and biomass generation with algae. In: Olivares, J.A.; Puyol, D.; Melero, J.A.; Dufour, J. Wastewater treatment residues as resources for biorefinery products and biofuels. Elsevier, pp. 229-254. https://doi.org/10.1016/B978-0-12-816204-0.00011-4.

American Public Health Association (APHA), 2012. Standard methods for the examination of water and wastewater. 22. ed. American Public Health Association, Washington, DC, 2012.

Barboza-Rodríguez, R.; Rodríguez-Jasso, R.M.; Rosero-Chasoy, G.; Rosales-Aguado, M.L.; Ruiz, H.A., 2024. Photobioreactor configurations in cultivating microalgae biomass for biorefinery. Bioresource Technology, v. 394, 130208. https://doi.org/10.1016/j.biortech.2023.130208.

Beltrán-Rocha, J.C.; Barceló-Quintal, I.D.; García-Martínez, M.; Osornio-Berthet, L.; Saavedra-Villarreal, N.; Villarreal-Chiu, J.; López-Chuken, U.J., 2017. Polishing of municipal secondary effluent using native microalgae consortia. Water Science and Technology, v. 75 (7), 1693-1701. https://doi.org/10.2166/wst.2017.046.

Bernard, O.; Rémond, B., 2012. Validation of a simple model accounting for light and temperature effect on microalgal growth. Bioresource Technology, v. 123, 520-527. https://doi.org/10.1016/j.biortech.2012.07.022.

Chia, S.R.; Chew, K.W.; Leong, H.Y.; Ho, S.H.; Munawaroh, H.S.H.; Show, P.L., 2021. CO2 mitigation and phycoremediation of industrial flue gas and wastewater via microalgae-bacteria consortium: possibilities and challenges. Chemical Engineering Journal, v. 425, 131436. https://doi.org/10.1016/j.cej.2021.131436.

Delgadillo-Mirquez, L.; Lopes, F.; Taidi, B.; Pareau, D., 2016. Nitrogen and phosphate removal from wastewater with a mixed microalgae and bacteria culture. Biotechnology Reports, v. 11, 18-26. https://doi.org/10.1016/j.btre.2016.04.003.

Gonçalves, A.L.; Pires, J.C.M.; Simões, M., 2017. A review on the use of microalgal consortia for wastewater treatment. Algal Research-Biomass Biofuels and Bioproducts, v. 24, 403-415. https://doi.org/10.1016/j.algal.2016.11.008.

Kaya, V.M.; Goulet, J.; de la Noüe, J.; Picard, G., 1996. Effect of intermittent CO2 enrichment during nutrient starvation on tertiary treatment of wastewater by alginate-immobilized *Scenedesmus bicellularis*. Enzyme and Microbial Technology, v. 18 (8), 550-554. https://doi.org/10.1016/0141-0229(95)00167-0.

Kube, M.; Jefferson, B.; Fan, L.; Roddick, F.A., 2018. The impact of wastewater characteristics, algal species selection and immobilisation on simultaneous nitrogen and phosphorus removal. Algal Research-Biomass Biofuels and Bioproducts, v. 31, 478-488. https://doi.org/10.1016/j.algal.2018.01.009.

Lee, Y.-J.; Lei, Z., 2019. Microalgal-bacterial aggregates for wastewater treatment: a mini-review. Bioresource Technology Reports, v. 8, 100199. https://doi.org/10.1016/j.biteb.2019.100199.

Li, Y.; Zhou, W.; Hu, B.; Min, M.; Chen, P.; Ruan, R., 2012. Effect of light intensity on algal biomass accumulation and biodiesel production for mixotrophic strains *Chlorella kessleri* and *Chlorella protothecoide* cultivated in highly concentrated municipal wastewater. Biotechnology and Bioengineering, v. 109 (9), 2222-2229. https://doi.org/10.1002/bit.24491.

Liu, X.; Ying, K.; Chen, G.; Zhou, C.; Zhang, W.; Zhang, X.; Cai, Z.; Holmes, T.; Tao, Y., 2017. 'Growth of Chlorella Vulgaris and Nutrient Removal in the Wastewater in Response to Intermittent Carbon Dioxide.' Chemosphere, v. 186, 977-985. https://doi.org/10.1016/j.chemosphere.2017.07.160.

Mayhead, E.; Silkina, A.; Llewellyn, C.A.; Fuentes-Grünewald, C.2018. Comparing nutrient removal from membrane filtered and unfiltered domestic wastewater using *Chlorella vulgaris*. Biology, v. 7 (1), 12. https://doi.org/10.3390/biology7010012.

Mohsenpour, S.F.; Hennige, S.; Willoughby, N.; Adeloye, A.; Gutierrez, T., 2021. Integrating micro-algae into wastewater treatment: a review. Science of The Total Environment, v. 752, 142168. https://doi.org/10.1016/j.scitotenv.2020.142168.

Mustafa, S.; Bhatti, H.N.; Maqbool, M.; Iqbal, M., 2021. Microalgae biosorption, bioaccumulation and biodegradation efficiency for the remediation of wastewater and carbon dioxide mitigation: prospects, challenges and opportunities. Journal of Water Process Engineering, v. 41, 102009. https://doi.org/10.1016/j.jwpe.2021.102009.

Yu, Q.; Pei, X.; Wei, Y.; Naveed, S.; Wang, S.; Chang, M.; Zhang, C.; Ge, Y., 2023. The roles of bacteria in resource recovery, wastewater treatment and carbon fixation by microalgae-bacteria consortia: a critical review. Algal Research, v. 69, 102938-102938. https://doi.org/10.1016/j.algal.2022.102938.

Pompei, C.M.E.; Bolzani, H.R.; da Silva, G.H.R., 2023. Use of native microalgae in anaerobic sewage treatment: lab and pilot-scale approaches. Journal of Applied Phycology, v. 35, 2865-2879. https://doi.org/10.1007/s10811-023-03081-1.

Ruas, G.; Serejo, M.L.; Paulo, P.L.; Boncz, M.Á., 2018. evaluation of domestic wastewater treatment using microalgal-bacterial processes: effect of CO2 addition on pathogen removal. Journal of Applied Psychology, v. 30 (2), 921-929. https://doi.org/10.1007/s10811-017-1280-6.

Silva, D.F.S.; Speranza, L.G.; Quartaroli, L.; Moruzzi, R.B.; Silva, G.H.R. da, 2020. Separation of microalgae cultivated in anaerobically digested black water using moringa oleifera lam seeds as coagulant. Journal of Water Process Engineering, v. 39, 101738. https://doi.org/10.1016/j.jwpe.2020.101738.

Silva, G.H.R. da; Sueitt, A.P.E.; Haimes, S.; Tripidaki, A.; van Zwieten, R.; Fernandes, T.V., 2019. Feasibility of closing nutrient cycles from black water by microalgae-based technology. Algal Research-Biomass Biofuels and Bioproducts, v. 44, 101715. https://doi.org/10.1016/j.algal.2019.101715.

Sirohi, R.; Pandey, A.K.; Ranganathan, P.; Singh, S.; Udayan, A.; Awasthi, M.A.; Hoang, A.T.; Chilakamarry, C.R.; Kim, S.H.; Sim, S.J., 2022. Design and applications of photobioreactors- a review. Bioresource Technology, v. 349, 126858. https://doi.org/10.1016/j.biortech.2022.126858.

Sutherland, D.L.; Ralph, P.J., 2019. Microalgal bioremediation of emerging contaminants - opportunities and challenges. Water Research, v. 164, 114921-114921. https://doi.org/10.1016/j.watres.2019.114921.

Torres-Franco, A.; Passos, F.; Figueredo, C., Mota, C.; Muñoz, R., 2021. Current advances in microalgae-based treatment of high-strength wastewaters: challenges and opportunities to enhance wastewater treatment performance. Reviews in Environmental Science and Bio/Technology, v. 20, 209-235. https://doi.org/10.1007/s11157-020-09556-8.

Wali, M.E.; Rahimpour Golroudbary, S.; Kraslawski, A., 2021. Circular economy for phosphorus supply chain and its impact on social sustainable development goals. Science of The Total Environment, v. 777, 146060-146060. https://doi.org/10.1016/j.scitotenv.2021.146060.

Zhang, B.; Li, W.; Guo, Y.; Zhang, Z.; Shi, W.; Cui, F.; Lens, P.N.L.; Tay, J.H., 2020. Microalgal-bacterial consortia: from interspecies interactions to biotechnological applications. Renewable & Sustainable Energy Reviews, v. 118, 109563. https://doi.org/10.1016/j.rser.2019.109563.